

## 3 The vector model

For most kinds of spectroscopy it is sufficient to think about energy levels and selection rules; this is not true for NMR. For example, using this energy level approach we cannot even describe how the most basic pulsed NMR experiment works, let alone the large number of subtle two-dimensional experiments which have been developed. To make any progress in understanding NMR experiments we need some more tools, and the first of these we are going to explore is the *vector model*.

This model has been around as long as NMR itself, and not surprisingly the language and ideas which flow from the model have become the language of NMR to a large extent. In fact, in the strictest sense, the vector model can only be applied to a surprisingly small number of situations. However, the ideas that flow from even this rather restricted area in which the model can be applied are carried over into more sophisticated treatments. It is therefore essential to have a good grasp of the vector model and how to apply it.

### 3.1 Bulk magnetization

We commented before that the nuclear spin has an interaction with an applied magnetic field, and that it is this which gives rise to the energy levels and ultimately an NMR spectrum. In many ways, it is permissible to think of the nucleus as behaving like a small bar magnet or, to be more precise, a *magnetic moment*. We will not go into the details here, but note that quantum mechanics tells us that the magnetic moment can be aligned in any direction<sup>1</sup>.

In an NMR experiment, we do not observe just one nucleus but a very large number of them (say  $10^{20}$ ), so what we need to be concerned with is the net effect of all these nuclei, as this is what we will observe.

If the magnetic moments were all to point in random directions, then the small magnetic field that each generates will cancel one another out and there will be no net effect. However, it turns out that at equilibrium the magnetic moments are not aligned randomly but in such a way that when their contributions are all added up there is a net magnetic field along the direction of the applied field ( $B_0$ ). This is called the *bulk magnetization* of the sample.

The magnetization can be represented by a vector – called the *magnetization vector* – pointing along the direction of the applied field ( $z$ ), as shown in Fig. 3.1. From now on we will only be concerned with what happens to this vector.

This would be a good point to comment on the axis system we are going to use – it is called a *right-handed set*, and such a set of axes is shown in Fig. 3.1. The name right-handed comes about from the fact that if you imagine grasping

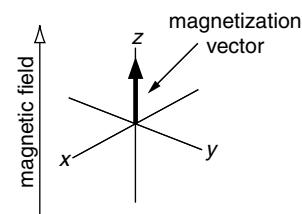


**Fig. 3.1** At equilibrium, a sample has a net magnetization along the magnetic field direction (the  $z$  axis) which can be represented by a magnetization vector. The axis set in this diagram is a right-handed one, which is what we will use throughout these lectures.

<sup>1</sup>It is a common misconception to state that the magnetic moment must either be aligned with or against the magnetic field. In fact, quantum mechanics says no such thing (see Levitt Chapter 9 for a very lucid discussion of this point).

the  $z$  axis with your right hand, your fingers curl from the  $x$  to the  $y$  axes.

### 3.2 Larmor precession

Suppose that we have managed, some how, to tip the magnetization vector away from the  $z$  axis, such that it makes an angle  $\beta$  to that axis. We will see later on that such a tilt can be brought about by a radiofrequency pulse. Once tilted away from the  $z$  axis we find is that the magnetization vector rotates about the direction of the magnetic field sweeping out a cone with a constant angle; see Fig. 3.2. The vector is said to *precesses* about the field and this particular motion is called *Larmor precession*.

If the magnetic field strength is  $B_0$ , then the frequency of the Larmor precession is  $\omega_0$  (in  $\text{rad s}^{-1}$ )

$$\omega_0 = -\gamma B_0$$

or if we want the frequency in Hz, it is given by

$$\nu_0 = -\frac{1}{2\pi}\gamma B_0$$

where  $\gamma$  is the gyromagnetic ratio. These are of course exactly the same frequencies that we encountered in section 2.3. In words, the frequency at which the magnetization precesses around the  $B_0$  field is exactly the same as the frequency of the line we see from the spectrum on one spin; this is no accident.

As was discussed in section 2.3, the Larmor frequency is a signed quantity and is negative for nuclei with a positive gyromagnetic ratio. This means that for such spins the precession frequency is negative, which is precisely what is shown in Fig. 3.2.

We can sort out positive and negative frequencies in the following way. Imagine grasping the  $z$  axis with your right hand, with the thumb pointing along the  $+z$  direction. The fingers then curl in the sense of a positive precession. Inspection of Fig. 3.2 will show that the magnetization vector is rotating in the opposite sense to your fingers, and this corresponds to a negative Larmor frequency.

### 3.3 Detection

The precession of the magnetization vector is what we actually detect in an NMR experiment. All we have to do is to mount a small coil of wire round the sample, with the axis of the coil aligned in the  $xy$ -plane; this is illustrated in Fig. 3.3. As the magnetization vector “cuts” the coil a current is induced which we can amplify and then record – this is the so-called *free induction* signal which is detected in a pulse NMR experiment. The whole process is analogous to the way in which electric current can be generated by a magnet rotating inside a coil.

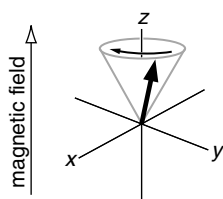


**Fig. 3.2** If the magnetization vector is tilted away from the  $z$  axis it executes a precessional motion in which the vector sweeps out a cone of constant angle to the magnetic field direction. The direction of precession shown is for a nucleus with a positive gyromagnetic ratio and hence a negative Larmor frequency.

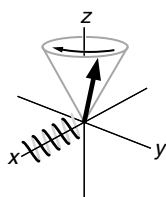


**Fig. 3.3** The precessing magnetization will cut a coil wound round the  $x$  axis, thereby inducing a current in the coil. This current can be amplified and detected; it is this that forms the free induction signal. For clarity, the coil has only been shown on one side of the  $x$  axis.

Essentially, the coil detects the  $x$ -component of the magnetization. We can easily work out what this will be. Suppose that the equilibrium magnetization vector is of size  $M_0$ ; if this has been tilted through an angle  $\beta$  towards the  $x$  axis, the  $x$ -component is  $M_0 \sin \beta$ ; Fig. 3.4 illustrates the geometry.

Although the magnetization vector precesses on a cone, we can visualize what happens to the  $x$ - and  $y$ -components much more simply by just thinking about the projection onto the  $xy$ -plane. This is shown in Fig. 3.5.

At time zero, we will assume that there is only an  $x$ -component. After a time  $\tau_1$  the vector has rotated through a certain angle, which we will call  $\epsilon_1$ . As the vector is rotating at  $\omega_0$  radians per second, in time  $\tau_1$  the vector has moved through  $(\omega_0 \times \tau_1)$  radians; so  $\epsilon_1 = \omega_0 \tau_1$ . At a later time, say  $\tau_2$ , the vector has had longer to precess and the angle  $\epsilon_2$  will be  $(\omega_0 \tau_2)$ . In general, we can see that after time  $t$  the angle is  $\epsilon = \omega_0 t$ .

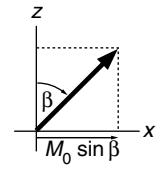


Fig. 3.4 Tilting the magnetization through an angle  $\theta$  gives an  $x$ -component of size  $M_0 \sin \beta$ .

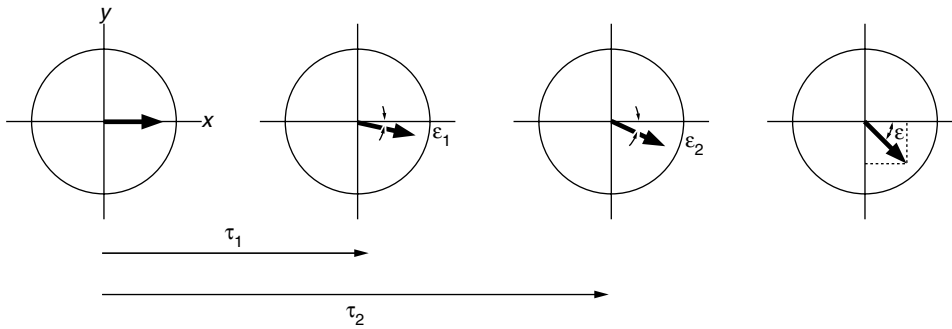


Fig. 3.5 Illustration of the precession of the magnetization vector in the  $xy$ -plane. The angle through which the vector has precessed is given by  $\omega_0 t$ . On the right-hand diagram we see the geometry for working out the  $x$  and  $y$  components of the vector.

We can now easily work out the  $x$ - and  $y$ -components of the magnetization using simple geometry; this is illustrated in Fig. 3.5. The  $x$ -component is proportional to  $\cos \epsilon$  and the  $y$ -component is negative (along  $-y$ ) and proportional to  $\sin \epsilon$ . Recalling that the initial size of the vector is  $M_0 \sin \beta$ , we can deduce that the  $x$ - and  $y$ -components,  $M_x$  and  $M_y$  respectively, are:

$$M_x = M_0 \sin \beta \cos(\omega_0 t)$$

$$M_y = -M_0 \sin \beta \sin(\omega_0 t).$$

Plots of these signals are shown in Fig. 3.6. We see that they are both simple oscillations at the Larmor frequency. Fourier transformation of these signals gives us the familiar spectrum – in this case a single line at  $\omega_0$ ; the details of how this works will be covered in a later chapter. We will also see in a later section that in practice we can easily detect *both* the  $x$ - and  $y$ -components of the magnetization.

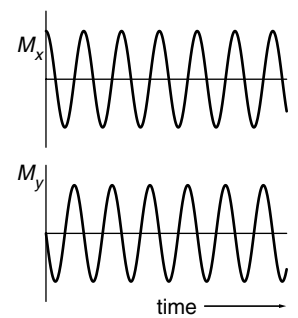


Fig. 3.6 Plots of the  $x$ - and  $y$ -components of the magnetization predicted using the approach of Fig. 3.5. Fourier transformation of these signals will give rise to the usual spectrum.

3.4 Pulses

We now turn to the important question as to how we can rotate the magnetization away from its equilibrium position along the  $z$  axis. Conceptually it is

easy to see what we have to do. All that is required is to (suddenly) replace the magnetic field along the  $z$  axis with one in the  $xy$ -plane (say along the  $x$  axis). The magnetization would then precess about the new magnetic field which would bring the vector down away from the  $z$  axis, as illustrated in Fig. 3.7.

Unfortunately it is all but impossible to switch the magnetic field suddenly in this way. Remember that the main magnetic field is supplied by a powerful superconducting magnet, and there is no way that this can be switched off; we will need to find another approach, and it turns out that the key is to use the idea of *resonance*.

The idea is to apply a very small magnetic field along the  $x$  axis but one which is oscillating at or near to the Larmor frequency – that is *resonant* with the Larmor frequency. We will show that this small magnetic field is able to rotate the magnetization away from the  $z$  axis, even in the presence of the very strong applied field,  $B_0$ .

Conveniently, we can use the same coil to generate this oscillating magnetic field as the one we used to detect the magnetization (Fig. 3.3). All we do is feed some radiofrequency (RF) power to the coil and the resulting oscillating current creates an oscillating magnetic field along the  $x$ -direction. The resulting field is called the *radiofrequency* or *RF field*. To understand how this weak RF field can rotate the magnetization we need to introduce the idea of the *rotating frame*.

### Rotating frame

When RF power is applied to the coil wound along the  $x$  axis the result is a magnetic field which oscillates along the  $x$  axis. The magnetic field moves back and forth from  $+x$  to  $-x$  passing through zero along the way. We will take the frequency of this oscillation to be  $\omega_{\text{RF}}$  (in  $\text{rad s}^{-1}$ ) and the size of the magnetic field to be  $2B_1$  (in T); the reason for the 2 will become apparent later. This frequency is also called the *transmitter frequency* for the reason that a radiofrequency transmitter is used to produce the power.

It turns out to be a lot easier to work out what is going on if we replace, in our minds, this *linearly* oscillating field with two counter-rotating fields; Fig. 3.8 illustrates the idea. The two counter rotating fields have the same magnitude  $B_1$ . One, denoted  $B_1^+$ , rotates in the positive sense (from  $x$  to  $y$ ) and the other, denoted  $B_1^-$ , rotates in the negative sense; both are rotating at the transmitter frequency  $\omega_{\text{RF}}$ .

At time zero, they are both aligned along the  $x$  axis and so add up to give a total field of  $2B_1$  along the  $x$  axis. As time proceeds, the vectors move away from  $x$ , in opposite directions. As the two vectors have the same magnitude and are rotating at the same frequency the  $y$ -components *always cancel* one another out. However, the  $x$ -components shrink towards zero as the angle through which the vectors have rotated approaches  $\frac{1}{2}\pi$  radians or  $90^\circ$ . As the angle increases beyond this point the  $x$ -component grows once more, but this time along the  $-x$  axis, reaching a maximum when the angle of rotation is  $\pi$ . The fields continue to rotate, causing the  $x$ -component to drop back to zero and rise again to a value  $2B_1$  along the  $+x$  axis. Thus we see that the two

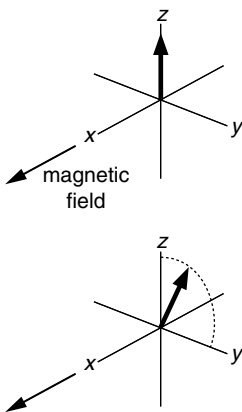


**Fig. 3.7** If the magnetic field along the  $z$  axis is replaced quickly by one along  $x$ , the magnetization will then precess about the  $x$  axis and so move towards the transverse plane.

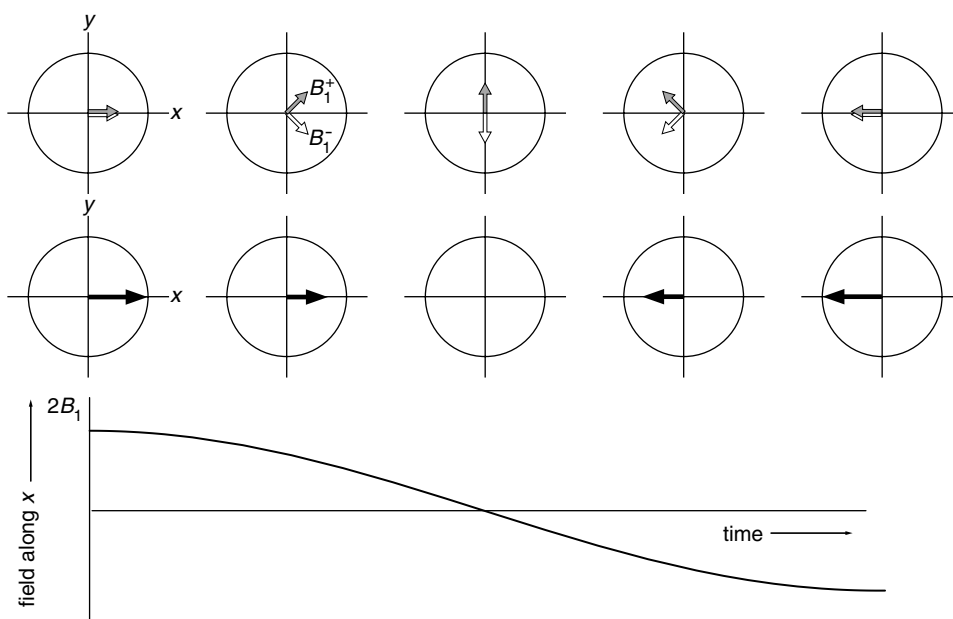


**Fig. 3.8** Illustration of how two counter-rotating fields (shown in the upper part of the diagram and marked  $B_1^+$  and  $B_1^-$ ) add together to give a field which is oscillating along the  $x$  axis (shown in the lower part). The graph at the bottom shows how the field along  $x$  varies with time.

counter-rotating fields add up to the linearly oscillating one.

Suppose now that we think about a nucleus with a positive gyromagnetic ratio; recall that this means the Larmor frequency is negative so that the sense of precession is from  $x$  towards  $-y$ . This is the same direction as the rotation of  $B_1^-$ . It turns out that the other field, which is rotating in the opposite sense to the Larmor precession, has no significant interaction with the magnetization and so from now on we will ignore it.

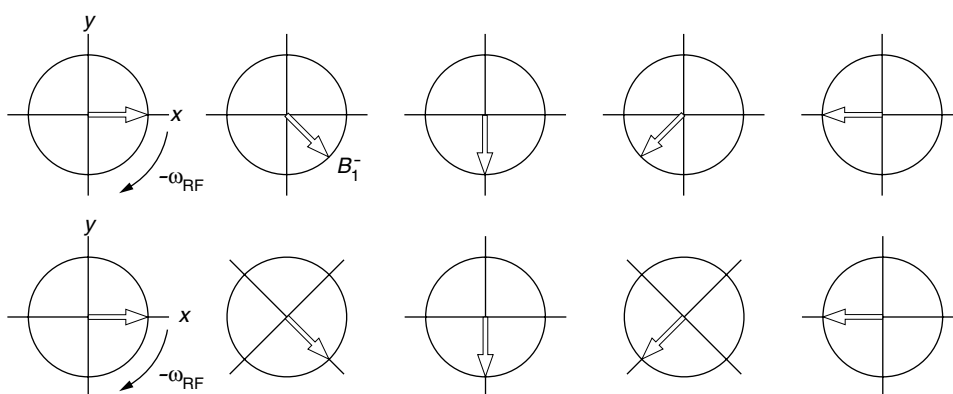


**Fig. 3.9** The top row shows a field rotating at  $-\omega_{RF}$  when viewed in a fixed axis system. The same field viewed in a set of axes rotating at  $-\omega_{RF}$  appears to be static.

We now employ a mathematical trick which is to move to a co-ordinate system which, rather than being static (called the *laboratory frame*) is rotating about the  $z$  axis in the same direction and at the same rate as  $B_1^-$  (i.e. at  $-\omega_{RF}$ ). In this rotating set of axes, or *rotating frame*,  $B_1^-$  appears to be static

and directed along the  $x$  axis of the rotating frame, as is shown in Fig. 3.9. This is a very nice result as the time dependence has been removed from the problem.

### Larmor precession in the rotating frame

We need to consider what happens to the Larmor precession of the magnetization when this is viewed in this rotating frame. In the fixed frame the precession is at  $\omega_0$ , but suppose that we choose the rotating frame to be at the same frequency. In the rotating frame the magnetization will appear *not to move* i.e. the apparent Larmor frequency will be zero! It is clear that moving to a rotating frame has an effect on the *apparent* Larmor frequency.

The general case is when the rotating frame is at frequency  $\omega_{\text{rot. fram.}}$ ; in such a frame the Larmor precession will appear to be at  $(\omega_0 - \omega_{\text{rot. fram.}})$ . This difference frequency is called the offset and is given the symbol  $\Omega$ :

$$\Omega = \omega_0 - \omega_{\text{rot. fram.}} \quad (3.1)$$

We have used several times the relationship between the magnetic field and the precession frequency:

$$\omega = -\gamma B. \quad (3.2)$$

From this it follows that if the apparent Larmor frequency in the rotating frame is different from that in fixed frame it must also be the case that the *apparent* magnetic field in the rotating frame must be different from the actual applied magnetic field. We can use Eq. 3.2 to compute the apparent magnetic field, given the symbol  $\Delta B$ , from the apparent Larmor frequency,  $\Omega$ :

$$\begin{aligned} \Omega &= -\gamma \Delta B \\ \text{hence } \Delta B &= -\frac{\Omega}{\gamma}. \end{aligned}$$

This apparent magnetic field in the rotating frame is usually called the *reduced field*,  $\Delta B$ .

If we choose the rotating frame to be at the Larmor frequency, the offset  $\Omega$  will be zero and so too will the reduced field. This is the key to how the very weak RF field can affect the magnetization in the presence of the much stronger  $B_0$  field. In the rotating frame this field along the  $z$  axis appears to shrink, and under the right conditions can become small enough that the RF field is dominant.

### The effective field

From the discussion so far we can see that when an RF field is being applied there are two magnetic fields in the rotating frame. First, there is the RF field (or  $B_1$  field) of magnitude  $B_1$ ; we will make this field static by choosing the rotating frame frequency to be equal to  $-\omega_{\text{RF}}$ . Second, there is the reduced field,  $\Delta B$ , given by  $(-\Omega/\gamma)$ . Since  $\Omega = (\omega_0 - \omega_{\text{rot. fram.}})$  and  $\omega_{\text{rot. fram.}} = -\omega_{\text{RF}}$  it follows that the offset is

$$\begin{aligned} \Omega &= \omega_0 - (-\omega_{\text{RF}}) \\ &= \omega_0 + \omega_{\text{RF}}. \end{aligned}$$

In this discussion we will assume that the gyromagnetic ratio is positive so that the Larmor frequency is negative.

This looks rather strange, but recall that  $\omega_0$  is negative, so if the transmitter frequency and the Larmor frequency are comparable the offset will be small.

In the rotating frame, the reduced field (which is along  $z$ ) and the RF or  $B_1$  field (which is along  $x$ ) add vectorially to give an effective field,  $B_{\text{eff}}$  as illustrated in Fig. 3.10. The size of this effective field is given by:

$$B_{\text{eff}} = \sqrt{B_1^2 + \Delta B^2}. \quad (3.3)$$

The magnetization precesses about this effective field at frequency  $\omega_{\text{eff}}$  given by

$$\omega_{\text{eff}} = \gamma B_{\text{eff}}$$

just in the same way that the Larmor precession frequency is related to  $B_0$ .

By making the offset small, or zero, the effective field lies close to the  $xy$ -plane, and so the magnetization will be rotated from  $z$  down to the plane, which is exactly what we want to achieve. The trick is that although  $B_0$  is much larger than  $B_1$  we can affect the magnetization with  $B_1$  by making it oscillate close to the Larmor frequency. This is the phenomena of resonance.

The angle between  $\Delta B$  and  $B_{\text{eff}}$  is called the *tilt angle* and is usually given the symbol  $\theta$ . From Fig. 3.10 we can see that:

$$\sin \theta = \frac{B_1}{B_{\text{eff}}} \quad \cos \theta = \frac{\Delta B}{B_{\text{eff}}} \quad \tan \theta = \frac{B_1}{\Delta B}.$$

All three definitions are equivalent.

### The effective field in frequency units

For practical purposes the thing that is important is the precession frequency about the effective field,  $\omega_{\text{eff}}$ . It is therefore convenient to think about the construction of the effective field not in terms of magnetic fields but in terms of the precession frequencies that they cause.

For each field the precession frequency is proportional to the magnetic field; the constant of proportion is  $\gamma$ , the gyromagnetic ratio. For example, we have already seen that in the rotating frame the apparent Larmor precession frequency,  $\Omega$ , depends on the reduced field:

$$\Omega = -\gamma \Delta B.$$

We define  $\omega_1$  as the precession frequency about the  $B_1$  field (the positive sign is intentional):

$$\omega_1 = \gamma B_1$$

and we already have

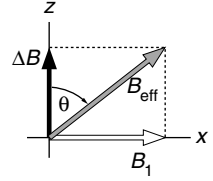
$$\omega_{\text{eff}} = \gamma B_{\text{eff}}.$$

Using these definitions in Eq. 3.3  $\omega_{\text{eff}}$  can be written as

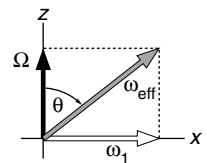
$$\omega_{\text{eff}} = \sqrt{\omega_1^2 + \Omega^2}.$$

Figure 3.10 can be redrawn in terms of frequencies, as shown in Fig. 3.11. Similarly, the tilt angle can be expressed in terms of these frequencies:

$$\sin \theta = \frac{\omega_1}{\omega_{\text{eff}}} \quad \cos \theta = \frac{\Omega}{\omega_{\text{eff}}} \quad \tan \theta = \frac{\omega_1}{\Omega}.$$



**Fig. 3.10** In the rotating frame the effective field  $B_{\text{eff}}$  is the vector sum of the reduced field  $\Delta B$  and the  $B_1$  field. The tilt angle,  $\theta$ , is defined as the angle between  $\Delta B$  and  $B_{\text{eff}}$ .



**Fig. 3.11** The effective field can be thought of in terms of frequencies instead of the fields used in Fig 3.10.

### On-resonance pulses

The simplest case to deal with is where the transmitter frequency is exactly the same as the Larmor frequency – it is said that the pulse is exactly *on resonance*. Under these circumstances the offset,  $\Omega$ , is zero and so the reduced field,  $\Delta B$ , is also zero. Referring to Fig. 3.10 we see that the effective field is therefore the same as the  $B_1$  field and lies along the  $x$  axis. For completeness we also note that the tilt angle,  $\theta$ , of the effective field is  $\pi/2$  or  $90^\circ$ .

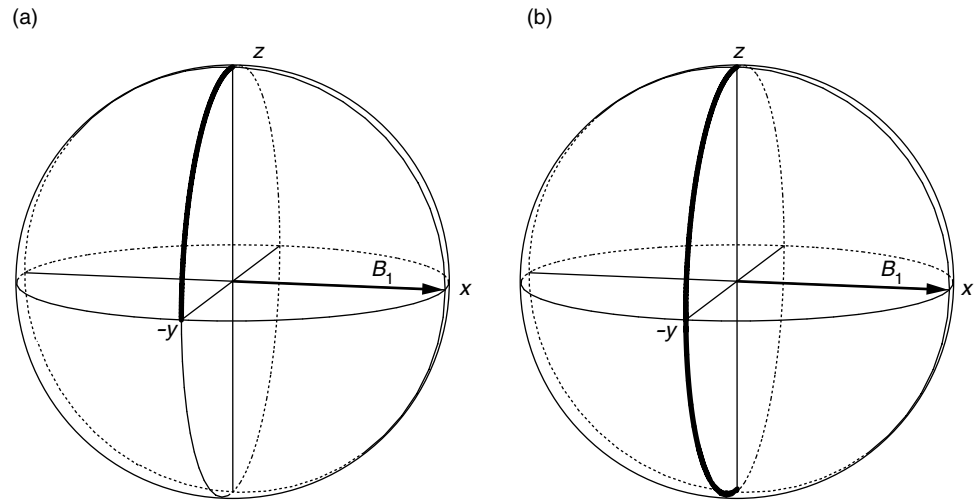


**Fig. 3.12** A “grapefruit” diagram in which the thick line shows the motion of a magnetization vector during an on-resonance pulse. The magnetization is assumed to start out along  $+z$ . In (a) the pulse flip angle is  $90^\circ$ . The effective field lies along the  $x$  axis and so the magnetization precesses in the  $yz$ -plane. The rotation is in the positive sense about  $x$  so the magnetization moves toward the  $-y$  axis. In (b) the pulse flip angle is  $180^\circ$  and so the magnetization ends up along  $-z$ .

In this situation the motion of the magnetization vector is very simple. Just as in Fig. 3.7 the magnetization precesses about the field, thereby rotating in the  $zy$ -plane. As we have seen above the precession frequency is  $\omega_1$ . If the RF field is applied for a time  $t_p$ , the angle,  $\beta$ , through which the magnetization has been rotated will be given by

$$\beta = \omega_1 t_p.$$

$\beta$  is called the *flip angle of the pulse*. By altering the time for which the pulse has been applied we can alter the angle through which the magnetization is rotated.

In many experiments the commonly used flip angles are  $\pi/2$  ( $90^\circ$ ) and  $\pi$  ( $180^\circ$ ). The motion of the magnetization vector during on-resonance  $90^\circ$  and  $180^\circ$  pulses are shown in Fig. 3.12. The  $90^\circ$  pulse rotates the magnetization from the equilibrium position to the  $-y$  axis; this is because the rotation is in the positive sense. Imagine grasping the axis about which the rotation is taking place (the  $x$  axis) with your right hand; your fingers then curl in the sense of a positive rotation.

If the pulse flip angle is set to  $180^\circ$  the magnetization is taken all the way from  $+z$  to  $-z$ ; this is called an *inversion pulse*. In general, for a flip angle  $\beta$



simple geometry tells us that the  $z$ - and  $y$ -components are

$$M_z = M_0 \cos \beta \quad M_y = -M_0 \sin \beta;$$

this is illustrated in Fig. 3.13.

### Hard pulses

In practical NMR spectroscopy we usually have several resonances in the spectrum, each of which has a different Larmor frequency; we cannot therefore be on resonance with all of the lines in the spectrum. However, if we make the RF field strong enough we can effectively achieve this condition.

By “hard” enough we mean that the  $B_1$  field has to be large enough that it is much greater than the size of the reduced field,  $\Delta B$ . If this condition holds, the effective field lies along  $B_1$  and so the situation is identical to the case of an on-resonance pulse. Thinking in terms of frequencies this condition translates to  $\omega_1$  being greater in magnitude than the offset,  $\Omega$ .

It is often relatively easy to achieve this condition. For example, consider a proton spectrum covering about 10 ppm; if we put the transmitter frequency at about 5 ppm, the maximum offset is 5 ppm, either positive or negative; this is illustrated in Fig. 3.14. If the spectrometer frequency is 500 MHz the maximum offset is  $5 \times 500 = 2500$  Hz. A typical spectrometer might have a  $90^\circ$  pulse lasting  $12 \mu\text{s}$ . From this we can work out the value of  $\omega_1$ . We start from

$$\beta = \omega_1 t_p \quad \text{hence} \quad \omega_1 = \frac{\beta}{t_p}.$$

We know that for a  $90^\circ$  pulse  $\beta = \pi/2$  and the duration,  $t_p$  is  $12 \times 10^{-6}$  s; therefore

$$\begin{aligned} \omega_1 &= \frac{\pi/2}{12 \times 10^{-6}} \\ &= 1.3 \times 10^5 \text{ rad s}^{-1}. \end{aligned}$$

The maximum offset is 2500 Hz, which is  $2\pi \times 2500 = 1.6 \times 10^4$  rad  $\text{s}^{-1}$ . We see that the RF field is about eight times the offset, and so the pulse can be regarded as strong over the whole width of the spectrum.

### 3.5 Detection in the rotating frame

To work out what is happening during an RF pulse we need to work in the rotating frame, and we have seen that to get this simplification the frequency of the rotating frame must match the transmitter frequency,  $\omega_{\text{RF}}$ . Larmor precession can be viewed just as easily in the laboratory and rotating frames; in the rotating frame the precession is at the offset frequency,  $\Omega$ .

It turns out that because of the way the spectrometer works the signal that we detect appears to be that in the rotating frame. So, rather than detecting an oscillation at the Larmor frequency, we see an oscillation at the offset,  $\Omega$ .<sup>2</sup>

<sup>2</sup>Strictly this is only true if we set the receiver reference frequency to be equal to the transmitter frequency; this is almost always the case. More details will be given in Chapter 5.

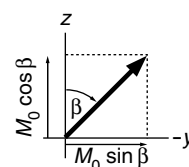


**Fig. 3.13** If the pulse flip angle is  $\beta$  we can use simple geometry to work out the  $y$ - and  $z$ -components.

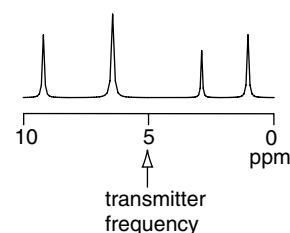


**Fig. 3.14** Illustration of the range of offsets one might see in a typical proton spectrum. If the transmitter frequency is placed as shown, the maximum offset of a resonance will be 5 ppm.

It also turns out that we can detect both the  $x$ - and  $y$ -components of the magnetization in the rotating frame. From now on we will work exclusively in the rotating frame.

### 3.6 The basic pulse–acquire experiment

At last we are in a position to describe how the simplest NMR experiment works – the one we use every day to record spectra. The experiment comes in three periods:

1. The sample is allowed to come to equilibrium.
2. RF power is switched on for long enough to rotate the magnetization through  $90^\circ$  i.e. a  $90^\circ$  pulse is applied.
3. After the RF power is switched off we start to detect the signal which arises from the magnetization as it rotates in the transverse plane.

The timing diagram – or *pulse sequence* as it is usually known – is shown in Fig. 3.15.

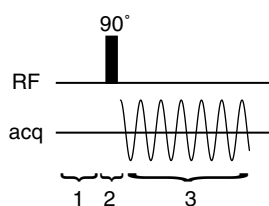


**Fig. 3.15** Timing diagram or pulse sequence for the simple pulse–acquire experiment. The line marked “RF” shows the location of the pulses, and the line marked “acq” shows when the signal is recorded or acquired.

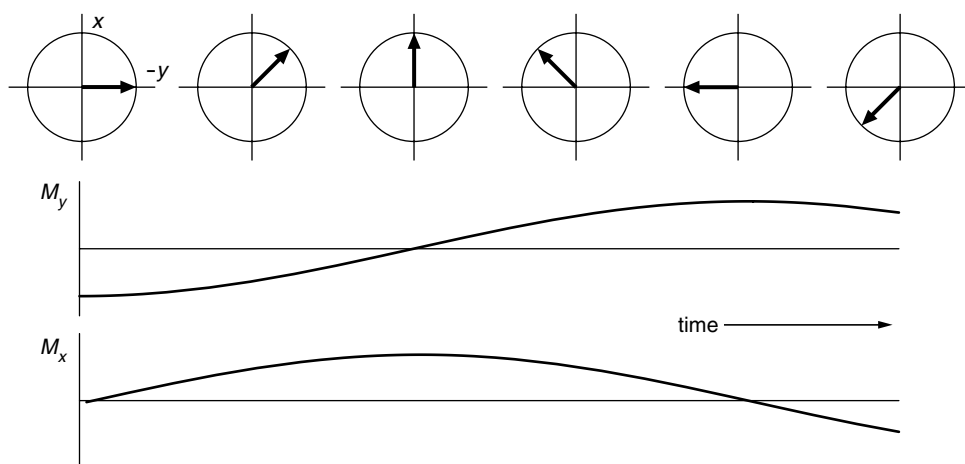


**Fig. 3.16** Evolution during the acquisition time (period 3) of the pulse–acquire experiment. The magnetization starts out along  $-y$  and evolves at the offset frequency,  $\Omega$  (here assumed to be positive). The resulting  $x$ - and  $y$ -magnetizations are shown below.

During period 1 equilibrium magnetization builds up along the  $z$  axis. As was described above, the  $90^\circ$  pulse rotates this magnetization onto the  $-y$  axis; this takes us to the end of period 2. During period 3 the magnetization precesses in the transverse plane at the offset  $\Omega$ ; this is illustrated in Fig. 3.16. Some simple geometry, shown in Fig. 3.17, enables us to deduce how the  $x$ - and  $y$ -magnetizations vary with time. The offset is  $\Omega$  so after time  $t$  the vector has precessed through an angle  $(\Omega \times t)$ . The  $y$ -component is therefore proportional to  $\cos \Omega t$  and the  $x$ -component to  $\sin \Omega t$ . In full the signals are:

$$M_y = -M_0 \cos(\Omega t)$$

$$M_x = M_0 \sin(\Omega t).$$

As we commented on before, Fourier transformation of these signals will give the usual spectrum, with a peak appearing at frequency  $\Omega$ .

### Spectrum with several lines

If the spectrum has more than one line, then to a good approximation we can associate a magnetization vector with each. Usually we wish to observe all the lines at once, so we choose the  $B_1$  field to be strong enough that for the range of offsets that these lines cover all the associated magnetization vectors will be rotated onto the  $-y$  axis. During the acquisition time each precesses at its own offset, so the detected signal will be:

$$M_y = -M_{0,1} \cos \Omega_1 t - M_{0,2} \cos \Omega_2 t - M_{0,3} \cos \Omega_3 t \dots$$

where  $M_{0,1}$  is the equilibrium magnetization of spin 1,  $\Omega_1$  is its offset and so on for the other spins. Fourier transformation of the free induction signal will produce a spectrum with lines at  $\Omega_1$ ,  $\Omega_2$  etc.

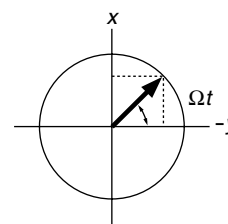


**Fig. 3.17** The magnetization starts out along the  $-y$  axis and rotates through an angle  $\Omega t$  during time  $t$ .

### 3.7 Pulse calibration

It is crucial that the pulses we use in NMR experiments have the correct flip angles. For example, to obtain the maximum intensity in the pulse-acquire experiment we must use a  $90^\circ$  pulse, and if we wish to invert magnetization we must use a  $180^\circ$  pulse. Pulse calibration is therefore an important preliminary to any experiment.

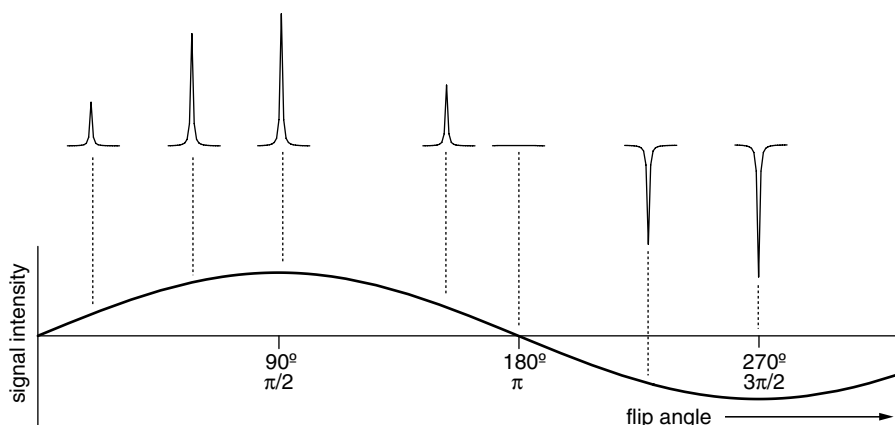


**Fig. 3.18** Illustration of how pulse calibration is achieved. The signal intensity varies as  $(\sin \beta)$  as shown by the curve at the bottom of the picture. Along the top are the spectra which would be expected for various different flip angles (indicated by the dashed lines). The signal is a maximum for a flip angle of  $90^\circ$  and goes through a null at  $180^\circ$ ; after that, the signal goes negative.

If we imagine an on-resonance or hard pulse we have already determined from Fig. 3.13 that the  $y$ -component of magnetization after a pulse of flip angle  $\beta$  is proportional to  $\sin \beta$ . If we therefore do a pulse-acquire experiment (section 3.6) and vary the flip angle of the pulse, we should see that the intensity of the signal varies as  $\sin \beta$ . A typical outcome of such an experiment is shown in Fig. 3.18.

The normal practice is to increase the flip angle until a null is found; the flip angle is then  $180^\circ$ . The reason for doing this is that the null is sharper than the maximum. Once the length of a  $180^\circ$  pulse is found, simply halving the time gives a  $90^\circ$  pulse.

Suppose that the  $180^\circ$  pulse was found to be of duration  $t_{180}$ . Since the flip angle is given by  $\beta = \omega_1 t_p$  we can see that for a  $180^\circ$  pulse in which the flip angle is  $\pi$

$$\pi = \omega_1 t_{180}$$

$$\text{hence } \omega_1 = \frac{\pi}{t_{180}}.$$

In this way we can determine  $\omega_1$ , usually called the RF *field strength* or the  $B_1$  *field strength*.

It is usual to quote the field strength not in  $\text{rad s}^{-1}$  but in Hz, in which case we need to divide by  $2\pi$ :

$$(\omega_1/2\pi) = \frac{1}{2t_{180}} \text{ Hz.}$$

For example, let us suppose that we found the null condition at  $15.5 \mu\text{s}$ ; thus

$$\omega_1 = \frac{\pi}{t_{180}} = \frac{\pi}{15.5 \times 10^{-6}} = 2.03 \times 10^5 \text{ rad s}^{-1}.$$

In frequency units the calculation is

$$(\omega_1/2\pi) = \frac{1}{2t_{180}} = \frac{1}{2 \times 15.5 \times 10^{-6}} = 32.3 \text{ kHz.}$$

In normal NMR parlance we would say “the  $B_1$  field is 32.3 kHz”. This is mixing the units up rather strangely, but the meaning is clear once you know what is going on!

### 3.8 The spin echo

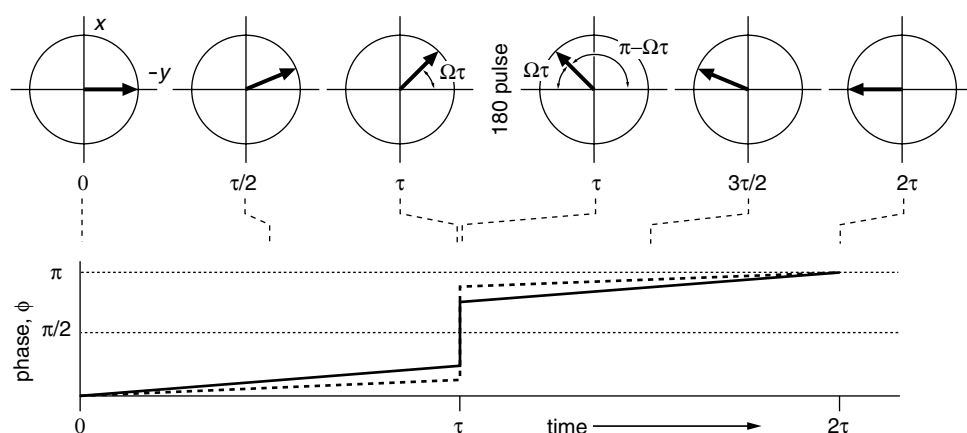


**Fig. 3.19** Vector diagrams showing how a spin echo refocuses the evolution of the offset; see text for details. Also shown is a phase evolution diagram for two different offsets (the solid and the dashed line).

We are now able to analyse the most famous pulsed NMR experiment, the *spin echo*, which is a component of a very large number of more complex experiments. The pulse sequence is quite simple, and is shown in Fig. 3.20. The special thing about the spin echo sequence is that at the end of the second  $\tau$  delay the magnetization ends up along the *same* axis, *regardless* of the values of  $\tau$  and the offset,  $\Omega$ .

We describe this outcome by saying that “the offset has been refocused”, meaning that at the end of the sequence it is just as if the offset had been zero and hence there had been no evolution of the magnetization. Figure 3.19 illustrates how the sequence works after the initial  $90^\circ$  pulse has placed the magnetization along the  $-y$  axis.

During the first delay  $\tau$  the vector precesses from  $-y$  towards the  $x$  axis. The angle through which the vector rotates is simply  $(\Omega t)$ , which we can describe as a *phase*,  $\phi$ . The effect of the  $180^\circ$  pulse is to move the vector to a mirror image position, with the mirror in question being in the  $xz$ -plane. So, the vector is now at an angle  $(\Omega\tau)$  to the  $y$  axis rather than being at  $(\Omega\tau)$  to the  $-y$  axis.

During the second delay  $\tau$  the vector continues to evolve; during this time it will rotate through a further angle of  $(\Omega\tau)$  and therefore at the end of the second delay the vector will be aligned along the  $y$  axis. A few moments thought will reveal that as the angle through which the vector rotates during the first  $\tau$  delay must be *equal* to that through which it rotates during the second  $\tau$  delay; the vector will therefore always end up along the  $y$  axis *regardless of the offset*,  $\Omega$ .

The  $180^\circ$  pulse is called a *refocusing pulse* because of the property that the evolution due to the offset during the first delay  $\tau$  is refocused during the second delay. It is interesting to note that the spin echo sequence gives exactly the same result as the sequence  $90^\circ - 180^\circ$  with the delays omitted.

Another way of thinking about the spin echo is to plot a phase evolution diagram; this is done at the bottom of Fig. 3.19. Here we plot the phase,  $\phi$ , as a function of time. During the first  $\tau$  delay the phase increases linearly with time. The effect of the  $180^\circ$  pulse is to change the phase from  $(\Omega\tau)$  to  $(\pi - \Omega\tau)$ ; this is the jump on the diagram at time  $\tau$ . Further evolution for time  $\tau$  causes the phase to increase by  $(\Omega\tau)$  leading to a final phase at the end of the second  $\tau$  delay of  $\pi$ . This conclusion is independent of the value of the offset  $\Omega$ ; the diagram illustrates this by the dashed line which represents the evolution of vector with a smaller offset.

As has already been mentioned, the effect of the  $180^\circ$  pulse is to reflect the vectors in the  $xz$ -plane. The way this works is illustrated in Fig. 3.21. The arc through which the vectors are moved is different for each, but all the vectors end up in mirror image positions.

### 3.9 Pulses of different phases

So far we have assume that the  $B_1$  field is applied along the  $x$  axis; this does not have to be so, and we can just as easily apply it along the  $y$  axis, for example. A pulse about  $y$  is said to be “phase shifted by  $90^\circ$ ” (we take an

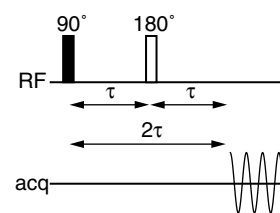


**Fig. 3.20** Pulse sequence for the *spin echo* experiment. The  $180^\circ$  pulse (indicated by an open rectangle as opposed to the closed one for a  $90^\circ$  pulse) is in the centre of a delay of duration  $2\tau$ , thus separating the sequence into two equal periods,  $\tau$ . The signal is acquired after the second delay  $\tau$ , or put another way, when the time from the beginning of the sequence is  $2\tau$ . The durations of the pulses are in practice very much shorter than the delays  $\tau$  but for clarity the length of the pulses has been exaggerated.

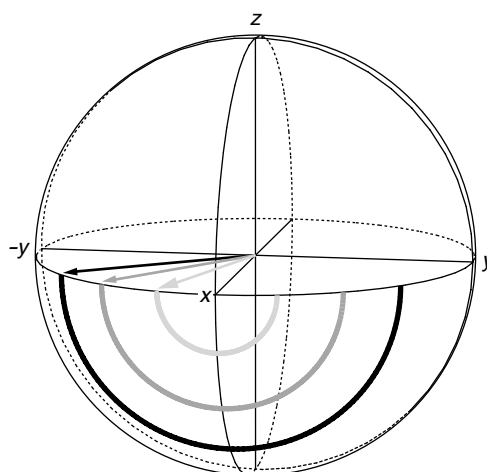


**Fig. 3.21** Illustration of the effect of a  $180^\circ$  pulse on three vectors which start out at different angles from the  $-y$  axis (coloured in black, grey and light grey). All three are rotated by  $180^\circ$  about the  $x$  axis on the trajectories indicated by the thick lines which dip into the southern hemisphere. As a result, the vectors end up in mirror image positions with respect to the  $xz$ -plane.

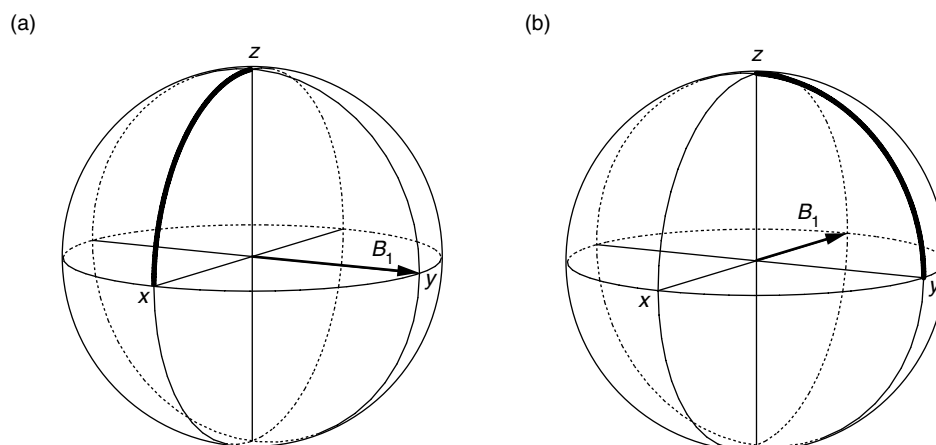


**Fig. 3.22** Grapefruit plots showing the effect on equilibrium magnetization of (a) a  $90^\circ$  pulse about the  $y$  axis and (b) a  $90^\circ$  pulse about the  $-x$  axis. Note the position of the  $B_1$  field in each case.

$x$ -pulse to have a phase shift of zero); likewise a pulse about  $-x$  would be said to be phase shifted by  $180^\circ$ . On modern spectrometers it is possible to produce pulses with arbitrary phase shifts.

If we apply a  $90^\circ$  pulse about the  $y$  axis to equilibrium magnetization we find that the vector rotates in the  $yz$ -plane such that the magnetization ends up along  $x$ ; this is illustrated in Fig. 3.22. As before, we can determine the effect of such a pulse by thinking of it as causing a positive rotation about the  $y$  axis. A  $90^\circ$  pulse about  $-x$  causes the magnetization to appear along  $y$ , as is also shown in Fig. 3.22.

We have seen that a  $180^\circ$  pulse about the  $x$  axis causes the vectors to move to mirror image positions with respect to the  $xz$ -plane. In a similar way,

a  $180^\circ$  pulse about the  $y$  axis causes the vectors to be reflected in the  $yz$ -plane.

### 3.10 Relaxation

We will have a lot more to say about relaxation later on, but at this point we will just note that the magnetization has a tendency to return to its equilibrium position (and size) – a process known as *relaxation*. Recall that the equilibrium situation has magnetization of size  $M_0$  along  $z$  and no transverse ( $x$  or  $y$ ) magnetization.

So, if we have created some transverse magnetization (for example by applying a  $90^\circ$  pulse) over time relaxation will cause this magnetization to decay away to zero. The free induction signal, which results from the magnetization precessing in the  $xy$  plane will therefore decay away in amplitude. This loss of  $x$ - and  $y$ -magnetization is called *transverse relaxation*.

Once perturbed, the  $z$ -magnetization will try to return to its equilibrium position, and this process is called *longitudinal relaxation*. We can measure the rate of this process using the *inversion recovery* experiment whose pulse sequence is shown in Fig. 3.23. The  $180^\circ$  pulse rotates the equilibrium magnetization to the  $-z$  axis. Suppose that the delay  $\tau$  is very short so that at the end of this delay the magnetization has not changed. Now the  $90^\circ$  pulse will rotate the magnetization onto the  $+y$  axis; note that this is in contrast to the case where the magnetization starts out along  $+z$  and it is rotated onto  $-y$ . If this gives a positive line in the spectrum, then having the magnetization along  $+y$  will give a negative line. So, what we see for short values of  $\tau$  is a negative line.

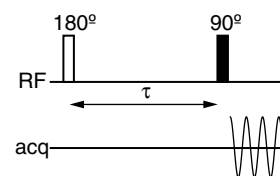


**Fig. 3.23** The pulse sequence for the inversion recovery experiment used to measure longitudinal relaxation.

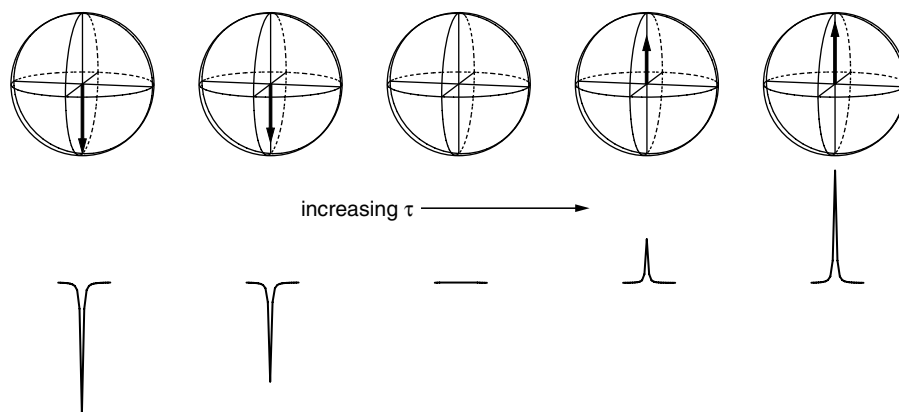


**Fig. 3.24** Visualization of the outcome of an inversion recovery experiment. The size and sign of the  $z$ -magnetization is reflected in the spectra (shown underneath). By analysing the peak heights as a function of the delay  $\tau$  it is possible to find the rate of recovery of the  $z$ -magnetization.

As  $\tau$  gets longer more relaxation takes place and the magnetization shrinks towards zero; this result is a negative line in the spectrum, but one whose size is decreasing. Eventually the magnetization goes through zero and then starts to increase along  $+z$  – this gives a positive line in the spectrum. Thus, by recording spectra with different values of the delay  $\tau$  we can map out the recovery of the  $z$ -magnetization from the intensity of the observed lines. The

whole process is visualized in Fig. 3.24.

### 3.11 Off-resonance effects and soft pulses

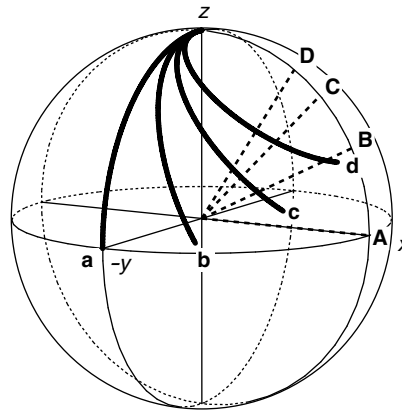


**Fig. 3.25** Grapefruit diagram showing the path followed during a pulse for various different resonance offsets. Path **a** is for the on-resonance case; the effective field lies along  $x$  and is indicated by the dashed line **A**. Path **b** is for the case where the offset is half the RF field strength; the effective field is marked **B**. Paths **c** and **d** are for offsets equal to and 1.5 times the RF field strength, respectively. The effective field directions are labelled **C** and **D**.

So far we have only dealt with the case where the pulse is either on resonance or where the RF field strength is large compared to the offset (a hard pulse) which is in effect the same situation. We now turn to the case where the offset is comparable to the RF field strength. The consequences of this are sometimes a problem to us, but they can also be turned to our advantage for *selective excitation*.

As the offset becomes comparable to the RF field, the effective field begins to move up from the  $x$  axis towards the  $z$  axis. As a consequence, rather than the magnetization moving in the  $yz$  plane from  $z$  to  $-y$ , the magnetization starts to follow a more complex curved path; this is illustrated in Fig. 3.25. The further off resonance we go, the further the vector ends up from the  $xy$  plane. Also, there is a significant component of magnetization generated along the  $x$  direction, something which does not occur in the on-resonance case.

We can see more clearly what is going on if we plot the  $x$  and  $y$  magnetization as a function of the offset; these are shown in Fig. 3.26. In (a) we see the  $y$ -magnetization and, as expected for a  $90^\circ$  pulse, on resonance the equilibrium magnetization ends up entirely along  $-y$ . However, as the offset increases the amount of  $y$ -magnetization generally decreases but imposed on this overall decrease there is an oscillation; at some offsets the magnetization is zero and at others it is positive. The plot of the  $x$ -magnetization, (b), shows a similar story with the magnetization generally falling off as the offset increases, but again with a strong oscillation.

Plot (c) is of the magnitude of the magnetization, which is given by

$$M_{\text{abs}} = \sqrt{M_x^2 + M_y^2}.$$



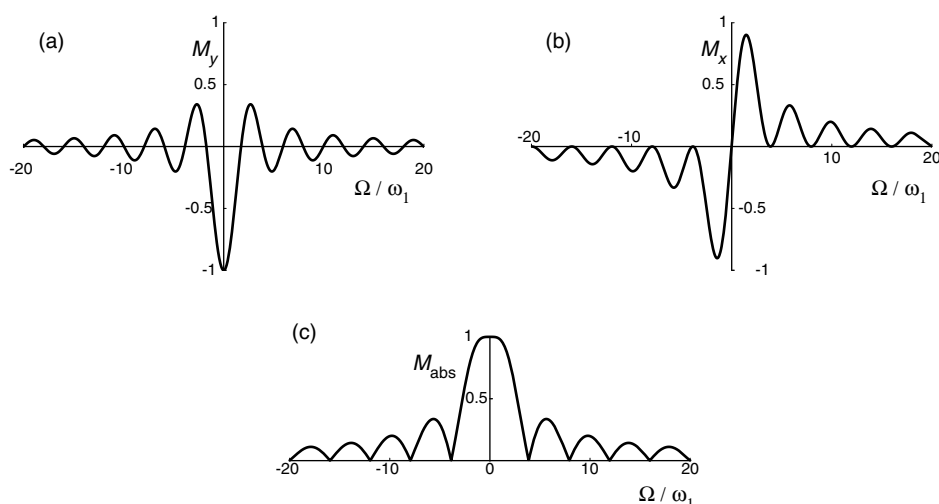


**Fig. 3.26** Plots of the magnetization produced by a pulse as a function of the offset. The pulse length has been adjusted so that on resonance the flip angle is  $90^\circ$ . The horizontal axes of the plots is the offset expressed as a ratio of the RF field strength,  $\omega_1$ ; the equilibrium magnetization has been assumed to be of size 1.

This gives the total transverse magnetization in any direction; it is, of course, always positive. We see from this plot the characteristic nulls and subsidiary maxima as the offset increases.

What plot (c) tells us is that although a pulse can excite magnetization over a wide range of offsets, the region over which it does so efficiently is really rather small. If we want at least 90% of the full intensity the offset must be less than about 1.6 times the RF field strength.

### Excitation of a range of shifts

There are some immediate practical consequences of this observation. Suppose that we are trying to record the full range of carbon-13 shifts (200 ppm) on a spectrometer whose magnetic field gives a proton Larmor frequency of 800 MHz and hence a carbon-13 Larmor frequency of 200 MHz. If we place the transmitter frequency at 100 ppm, the maximum offset that a peak can have is 100 ppm which, at this Larmor frequency, translates to 20 kHz. According to our criterion above, if we accept a reduction to 90% of the full intensity at the edges of the spectrum we would need an RF field strength of  $20/1.6 \approx 12.5$  kHz. This would correspond to a  $90^\circ$  pulse width of  $20 \mu\text{s}$ . If the manufacturer failed to provide sufficient power to produce this pulse width we can see that the excitation of the spectrum will fall below our (arbitrary) 90% mark.

We will see in a later section that the presence of a mixture of  $x$ - and  $y$ -magnetization leads to phase errors in the spectrum which can be difficult to correct.

### Selective excitation

Sometimes we want to excite just a portion of the spectrum, for example just the lines of a single multiplet. We can achieve this by putting the transmitter in the centre of the region we wish to excite and then reducing the RF field

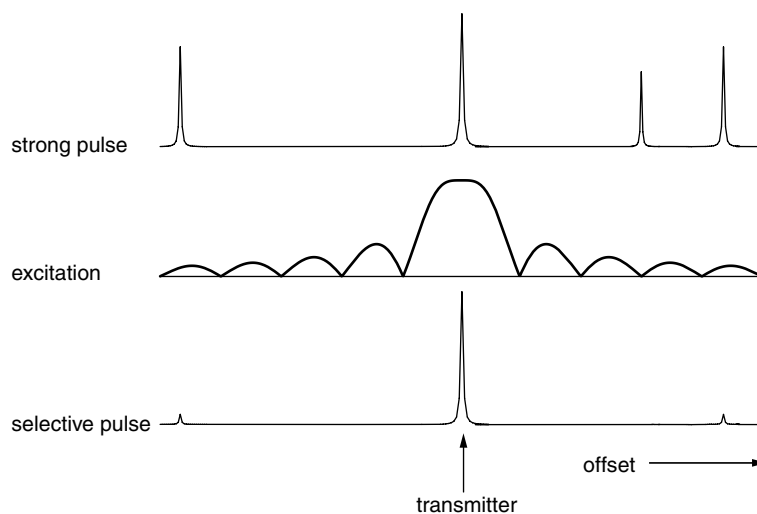


**Fig. 3.27** Visualization of the use of selective excitation to excite just one line in the spectrum. At the top is shown the spectrum that would be excited using a hard pulse. If the transmitter is placed on resonance with one line and the strength of the RF field reduced then the pattern of excitation we expect is as shown in the middle. As a result, the peaks at non-zero offsets are attenuated and the spectrum which is excited will be as shown at the bottom.

strength until the degree of excitation of the rest of the spectrum is essentially negligible. Of course, reducing the RF field strength lengthens the duration of a  $90^\circ$  pulse. The whole process is visualized in Fig. 3.27.

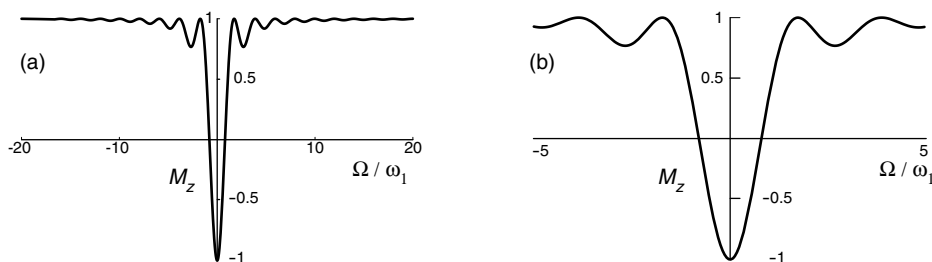
Such pulses which are designed to affect only part of the spectrum are called *selective pulses* or *soft pulses* (as opposed to non-selective or hard pulses). The value to which we need to reduce the RF field depends on the separation of the peak we want to excite from those we do not want to excite. The closer in the unwanted peaks are the weaker the RF field must become and hence the longer the  $90^\circ$  pulse. In the end a balance has to be made between making the pulse too long (and hence losing signal due to relaxation) and allowing a small amount of excitation of the unwanted signals.

Figure 3.27 does not portray one problem with this approach, which is that for peaks away from the transmitter a mixture of  $x$ - and  $y$ -magnetization is generated (as shown in Fig. 3.26). This is described as a phase error, more of which in a later section. The second problem that the figure does show is that the excitation only falls off rather slowly and “bounces” through a series of maximum and nulls; these are sometimes called “wiggles”. We might be lucky and have an unwanted peak fall on a null, or unlucky and have an unwanted peak fall on a maximum.

Much effort has been put into getting round both of these problems. The key feature of all of the approaches is to “shape” the envelope of the RF pulses i.e. not just switch it on and off abruptly, but with a smooth variation. Such pulses are called *shaped pulses*. The simplest of these are basically bell-shaped (like a gaussian function, for example). These suppress the “wiggles” at large offsets and give just a smooth decay; they do not, however, improve the phase properties. To attack this part of the problem requires an altogether more sophisticated approach.

### Selective inversion

Sometimes we want to invert the magnetization associated with just one resonance while leaving all the others in the spectrum unaffected; such a pulse would be called a *selective inversion* pulse. Just as for selective excitation, all we need to do is to place the transmitter on the line we wish to invert and reduce the RF field until the other resonances in the spectrum are not affected significantly. Of course we need to adjust the pulse duration so that the on-resonance flip angle is  $180^\circ$ .



**Fig. 3.28** Plots of the  $z$ -magnetization produced by a pulse as a function of the offset; the flip angle on-resonance has been set to  $180^\circ$ . Plot (b) covers a narrower range of offsets than plot (a). These plots should be compared with those in Fig. 3.26.

Figure 3.28 shows the  $z$ -magnetization generated as a function of offset for a pulse. We see that the range over which there is significant inversion is rather small, and that the oscillations are smaller in amplitude than for the excitation pulse.

This observation has two consequences: one “good” and one “bad”. The good consequence is that a selective  $180^\circ$  pulse is, for a given field strength, more selective than a corresponding  $90^\circ$  pulse. In particular, the weaker “bouncing” sidelobes are a useful feature. Do not forget, though, that the  $180^\circ$  pulse is longer, so some of the improvement may be illusory!

The bad consequence is that when it comes to hard pulses the range of offsets over which there is anything like complete inversion is much more limited than the range of offsets over which there is significant excitation. This can be seen clearly by comparing Fig. 3.28 with Figure 3.26. Thus,  $180^\circ$  pulses are often the source of problems in spectra with large offset ranges.

### 3.12 Exercises

#### E 3-1

A spectrometer operates with a Larmor frequency of 600 MHz for protons. For a particular set up the RF field strength,  $\omega_1/(2\pi)$  has been determined to be 25 kHz. Suppose that the transmitter is placed at 5 ppm; what is the offset (in Hz) of a peak at 10 ppm? Compute the tilt angle,  $\theta$ , of a spin with this offset.

For the normal range of proton shifts (0 – 10 ppm), is this 25 kHz field strong enough to give what could be classed as hard pulses?

#### E 3-2

In an experiment to determine the pulse length an operator observed a positive signal for pulse widths of 5 and 10  $\mu\text{s}$ ; as the pulse was lengthened further the intensity decreased going through a null at 20.5  $\mu\text{s}$  and then turning negative.

Explain what is happening in this experiment and use the data to determine the RF field strength in Hz and the length of a  $90^\circ$  pulse.

A further null in the signal was seen at 41.0  $\mu\text{s}$ ; to what do you attribute this?

#### E 3-3

Use vector diagrams to describe what happens during a spin echo sequence in which the  $180^\circ$  pulse is applied about the  $y$  axis. Also, draw a phase evolution diagram appropriate for this pulse sequence.

In what way is the outcome different from the case where the refocusing pulse is applied about the  $x$  axis?

What would the effect of applying the refocusing pulse about the  $-x$  axis be?

#### E 3-4

The gyromagnetic ratio of phosphorus-31 is  $1.08 \times 10^8 \text{ rad s}^{-1} \text{ T}^{-1}$ . This nucleus shows a wide range of shifts, covering some 700 ppm.

Estimate the minimum  $90^\circ$  pulse width you would need to excite peaks in this complete range to within 90% of their theoretical maximum for a spectrometer with a  $B_0$  field strength of 9.4 T.

#### E 3-5

A spectrometer operates at a Larmor frequency of 400 MHz for protons and hence 100 MHz for carbon-13. Suppose that a  $90^\circ$  pulse of length 10  $\mu\text{s}$  is applied to the protons. Does this have a significant effect of the carbon-13 nuclei? Explain your answer carefully.

#### E 3-6

Referring to the plots of Fig. 3.26 we see that there are some offsets at which the transverse magnetization goes to zero. Recall that the magnetization is rotating about the *effective field*,  $\omega_{\text{eff}}$ ; it follows that these nulls in the excitation

come about when the magnetization executes complete  $360^\circ$  rotations about the effective field. In such a rotation the magnetization is returned to the  $z$  axis. Make a sketch of a “grapefruit” showing this.

The effective field is given by

$$\omega_{\text{eff}} = \sqrt{\omega_1^2 + \Omega^2}.$$

Suppose that we express the offset as a multiple  $\kappa$  of the RF field strength:

$$\Omega = \kappa \omega_1.$$

Show that with this values of  $\Omega$  the effective field is given by:

$$\omega_{\text{eff}} = \omega_1 \sqrt{1 + \kappa^2}.$$

(The reason for doing this is to reduce the number of variables.)

Let us assume that on-resonance the pulse flip angle is  $\pi/2$ , so the duration of the pulse,  $\tau_p$ , is give from

$$\omega_1 \tau_p = \pi/2 \quad \text{thus} \quad \tau_p = \frac{\pi}{2\omega_1}.$$

The angle of rotation about the effective field for a pulse of duration  $\tau_p$  is  $(\omega_{\text{eff}}\tau_p)$ . Show that for the effective field given above this angle,  $\beta_{\text{eff}}$  is given by

$$\beta_{\text{eff}} = \frac{\pi}{2} \sqrt{1 + \kappa^2}.$$

The null in the excitation will occur when  $\beta_{\text{eff}}$  is  $2\pi$  i.e. a complete rotation. Show that this occurs when  $\kappa = \sqrt{15}$  i.e. when  $(\Omega/\omega_1) = \sqrt{15}$ . Does this agree with Fig. 3.26?

Predict other values of  $\kappa$  at which there will be nulls in the excitation.

### E 3-7

When calibrating a pulse by looking for the null produced by a  $180^\circ$  rotation, why is it important to choose a line which is close to the transmitter frequency (i.e. one with a small offset)?

### E 3-8

Use vector diagrams to predict the outcome of the sequence:

$$90^\circ - \text{delay } \tau - 90^\circ$$

applied to equilibrium magnetization; both pulses are about the  $x$  axis. In your answer, explain how the  $x$ ,  $y$  and  $z$  magnetizations depend on the delay  $\tau$  and the offset  $\Omega$ .

### E 3-9

Consider the spin echo sequence to which a  $90^\circ$  pulse has been added at the end:

$$90^\circ(x) - \text{delay } \tau - 180^\circ(x) - \text{delay } \tau - 90^\circ(\phi).$$

The axis about which the pulse is applied is given in brackets after the flip angle. Explain in what way the outcome is different depending on whether the phase  $\phi$  of the pulse is chosen to be  $x$ ,  $y$ ,  $-x$  or  $-y$ .

### E 3-10

The so-called “1- $\bar{1}$ ” sequence is:

$$90^\circ(x) - \text{delay } \tau - 90^\circ(-x)$$

For a peak which is on resonance the sequence does not excite any observable magnetization. However, for a peak with an offset such that  $\Omega\tau = \pi/2$  the sequence results in all of the equilibrium magnetization appearing along the  $x$  axis. Further, if the delay is such that  $\Omega\tau = \pi$  no transverse magnetization is excited.

Explain these observations and make a sketch graph of the amount of transverse magnetization generated as a function of the offset for a fixed delay  $\tau$ .

The sequence has been used for suppressing strong solvent signals which might otherwise overwhelm the spectrum. The solvent is placed on resonance, and so is not excited;  $\tau$  is chosen so that the peaks of interest are excited. How does one go about choosing the value for  $\tau$ ?

### E 3-11

The so-called “1-1” sequence is:

$$90^\circ(x) - \text{delay } \tau - 90^\circ(y).$$

Describe the excitation that this sequence produces as a function of offset. How it could be used for observing spectra in the presence of strong solvent signals?